

NEW OBSERVATIONS OF THE VERY LUMINOUS SUPERNOVA 2006GY: EVIDENCE FOR ECHOES

A. A. MILLER¹, N. SMITH¹, W. LI¹, J. S. BLOOM^{1,2}, R. CHORNOCK¹, A. V. FILIPPENKO¹, AND J. X. PROCHASKA^{3,4}

Draft version November 16, 2018

ABSTRACT

Supernova (SN) 2006gy was a hydrogen-rich core-collapse SN that remains one of the most luminous optical supernovae ever observed. The total energy budget ($> 2 \times 10^{51}$ erg radiated in the optical alone) poses many challenges for standard SN theory. We present new ground-based near-infrared (NIR) observations of SN 2006gy, as well as a single epoch of *Hubble Space Telescope* (*HST*) imaging obtained more than two years after the explosion. Our NIR data taken around peak optical emission show an evolution that is largely consistent with a cooling blackbody, with tentative evidence for a growing NIR excess starting around day ~ 130 . Our late-time Keck adaptive optics NIR image, taken on day 723, shows little change from previous NIR observations taken around day 400. Furthermore, the optical *HST* observations show a reduced decline rate after day 400, and the SN is bluer on day 810 than it was at peak. This late-time decline is inconsistent with ^{56}Co decay, and thus is problematic for the various pair-instability SN models used to explain the nature of SN 2006gy. The slow decline of the NIR emission can be explained with a light echo, and we confirm that the late-time NIR excess is the result of a massive ($\gtrsim 10 M_{\odot}$) dusty shell heated by the SN peak luminosity. The late-time optical observations require the existence of a scattered light echo, which may be generated by the same dust that contributes to the NIR echo. Both the NIR and optical echoes originate in the proximity of the progenitor, $\sim 10^{18}$ cm for the NIR echo and $\lesssim 10\text{--}40$ pc for the optical echo, which provides further evidence that the progenitor of SN 2006gy was a very massive star.

Subject headings: supernovae: general — supernovae: individual (SN 2006gy)

1. INTRODUCTION

At the time of discovery, supernova (SN) 2006gy was the most luminous SN ever found (Ofek et al. 2007; Smith et al. 2007). SN 2006gy generated a great deal of interest; in addition to being ~ 100 times more luminous than a typical Type II (hydrogen-rich, core-collapse) SN at peak, it exhibited a long rise time (~ 70 day) and slow decline, leading to speculation that it may have been the first observed example of a pair-instability SN (PISN; Ofek et al. 2007; Smith et al. 2007)⁵ or a pulsational pair-instability SN (Woosley, Blinnikov, & Heger 2007).

SN 2006gy was classified as a Type IIn SN (see Schlegel 1990 for a definition of the Type IIn subclass and Filippenko 1997 for a review of its spectral properties) based on the relatively narrow emission features present in the early-time SN spectrum. Some Type IIn supernovae (SNe IIn) are known to be overluminous relative to their typical SN II counterparts: $M_R \approx -15.8$ mag for Type II-P with a 1σ scatter of 1.1 mag (Li et al. 2010), whereas SN 2006gy reached $M_R \approx -21.7$ mag. The enhanced luminosity of some SNe IIn is probably due to the collision of fast-moving SN ejecta with a dense, and possibly clumpy, circumstellar medium (CSM; e.g., Chugai & Danziger 1994). In a companion paper (Smith et al. 2010), a detailed spectroscopic

comparison of SN 2006gy is made to other SNe IIn. SN 2006gy is unique within the SN IIn subclass, however, because typical interaction models cannot explain its early-time behavior, suggesting the need for alternative models for this particular object (Smith et al. 2007; Woosley, Blinnikov, & Heger 2007; Nomoto et al. 2007; Smith et al. 2010).

Pair-instability SNe (Barkat, Rakavy, & Sack 1967; Rakavy & Shaviv 1967; Bond, Arnett, & Carr 1984) are expected to occur in very massive, low-metallicity stars, such as those that may have been present in the metal-free environment of the very early universe (e.g., Abel, Bryan, & Norman 2000). The detection of a pair-instability SN in the comparatively local universe, then, could potentially reveal a great deal about the first generation of stars. The light curves of pair-instability SNe are expected to exhibit a relatively slow rise, followed by a broad turnover after the peak, and a peak luminosity that is considerably larger than that of typical SNe (Scannapieco et al. 2005). Qualitatively, each of these characteristics matches those observed for SN 2006gy.

Other more luminous SNe have been announced since the discovery of SN 2006gy: SNe 2005ap (Quimby et al. 2007) and 2008es (Miller et al. 2009; Gezari et al. 2009). This suggests that while these events are rare, there may be a new subclass of very luminous supernovae (VLSNe). The peak luminosity and photometric evolution of both SNe 2005ap and 2008es are difficult to explain via the pair-instability model (Quimby et al. 2007; Miller et al. 2009), implying that peak luminosities $\gtrsim \text{few} \times 10^{44}$ erg s⁻¹ are possible without a pair-instability explosion. There is a wide diversity of alternative models that have been developed to explain the early-time observations of SN 2006gy. Smith & McCray (2007) argue that the peak

¹ Department of Astronomy, University of California, Berkeley, CA 94720-3411.

² Sloan Research Fellow.

³ University of California Observatories/Lick Observatory, University of California, Santa Cruz, CA 95064.

⁴ Department of Astronomy and Astrophysics, University of California, Santa Cruz, CA 95064.

⁵ Currently, there is much stronger evidence that SN 2007bi is the first observed example of a PISN (Gal-Yam et al. 2009).

luminosity and light-curve evolution can be explained via the thermalization of shock energy deposited into a massive ($\sim 10 M_{\odot}$), optically thick shell. Based on a model of the light curve near peak, Agnoletto et al. (2009) suggest that the combination of ejecta colliding with dense clumps in the CSM and $\sim 1\text{--}3 M_{\odot}$ of ^{56}Ni are responsible for the early-time luminosity of SN 2006gy. Nomoto et al. (2007) are unable to match the light curve with a standard pair-instability SN model; however, they can reasonably reproduce the ($\lesssim 400$ day) light curve of SN 2006gy using a pair-instability model where they artificially reduce the ejecta mass, such that the radioactive heating is less than 100% efficient. The reduction in ejecta mass should lead to a reduction in ^{56}Ni production, as noted by Nomoto et al. (2007); thus, their model with an artificially reduced ejecta mass may not be self-consistent. Woosley, Blinnikov, & Heger (2007) use a model of a pulsational pair instability within a massive star to explain the light curve of SN 2006gy.

Some of the models make predictions for the late-time behavior of SN 2006gy. Those with a large yield of ^{56}Ni (Nomoto et al. 2007; Smith et al. 2007) would expect a decline in bolometric luminosity at the rate of ^{56}Co decay, $0.98 \text{ mag } (100 \text{ day})^{-1}$, or faster if the radioactive-decay energy is not converted to optical emission with 100% efficiency. The shell-shock model (Smith & McCray 2007) predicts a rapid decline after ~ 200 day, though the authors note that this decline may be offset by the production of a large amount of ^{56}Ni or continued CSM interaction. The pulsational pair-instability model (Woosley, Blinnikov, & Heger 2007) predicts another SN explosion at the location of SN 2006gy about 9 years after the initial outburst from SN 2006gy.

More than a year after the explosion, Smith et al. (2008b) detected SN 2006gy in the near infrared (NIR) at a luminosity comparable to that of the peak luminosity of most SNe II. This property had not been predicted by any of the models. When coupled with the lack of a detection in the radio and X-rays, this led Smith et al. (2008b) to conclude that the luminosity could not be powered by the continued interaction of the SN ejecta with CSM. Kawabata et al. (2009) draw similar conclusions based on their detection of weak $H\alpha$ emission at a comparable epoch. Smith et al. (2008b) conclude that only two possibilities are able to explain the late-time observations of SN 2006gy: (i) the explosion produced $\gtrsim 2.5 M_{\odot}$ of ^{56}Ni , which is only theoretically expected for PISNe (e.g., Scannapieco et al. 2005), which was heating dust and consequently generating the large NIR excess, or (ii) a massive ($\sim 5\text{--}10 M_{\odot}$), dusty shell, located ~ 1 light year from the site of the SN, was being heated by the radiation produced at peak, and reradiating that energy as a NIR echo (Dwek 1983). For the first case, if the luminosity were powered by radioactive decay, then future observations should indicate a continued decline at the rate of ^{56}Co decay. A dust echo, on the other hand, would result in a NIR light curve that stays roughly constant for $\sim 1\text{--}2$ yr before exhibiting a rapid decline.

Evolved massive stars, such as red supergiants and luminous blue variables (LBVs), are often observed to have massive dust shells, so if these stars explode as SNe II one might expect a late-time IR echo. Many

SNe II have been observed to exhibit a late-time NIR excess (Gerardy et al. 2002) which in some cases lasted > 1 yr. This excess has been attributed to NIR echoes (Gerardy et al. 2002), though we note that the formation of new dust has been argued specifically for SN 1998S (Pozzo et al. 2004) and SN 1995N (Fox et al. 2009). Dusty regions near the SN should also lead to ultraviolet (UV) and optical scattered-light echoes (Chevalier 1986); thus, dust is capable of providing significant optical and NIR emission at late times. The optical decline of SNe II at late times is very heterogeneous (Li et al. 2002), and therefore caution must be applied when determining the source of any late-time emission.

In this paper we present new NIR observations of SN 2006gy, taken around the peak of optical emission, as well as optical and NIR observations obtained more than two years after SN 2006gy exploded. Section 2 describes the observations and data reduction. We discuss the results in § 3, and in § 4 we offer some conclusions. Throughout this paper we assume that the distance to NGC 1260 (the host galaxy of SN 2006gy) is 73.1 Mpc, and following Smith et al. (2007) we adopt $E(B-V) = 0.54$ mag as the reddening toward SN 2006gy within the host galaxy, while Galactic extinction accounts for $E(B-V) = 0.18$ mag, leading to a total color excess toward SN 2006gy of $E(B-V) = 0.72$ mag. All spectral energy distributions (SEDs) have been corrected for this color excess assuming $R_V = A_V/E(B-V) = 3.1$ using the reddening law of Cardelli, Clayton, & Mathis (1989).

2. OBSERVATIONS

NIR observations of SN 2006gy were obtained simultaneously in J , H , and K_s with the Peters Automated Infrared Imaging Telescope (PAIRITEL; Bloom et al. 2006) starting on 2006 October 13 UT⁶ (54 days after explosion⁷). PAIRITEL is a 1.3-m robotic telescope, located on Mt. Hopkins, AZ, which obtained images over the next 24 months for 0.5–1 hr at each of the 124 epochs through normal queue-scheduled operations. All images were processed via an automated pipeline (Bloom et al. 2006).

Analysis of SN 2006gy has proved challenging because the SN is located very close to the nucleus of NGC 1260 (separation $\sim 1''$; Ofek et al. 2007; Smith et al. 2007). PAIRITEL has a large native scale of $2'' \text{ pixel}^{-1}$, precluding spatial resolution of the SN from the nucleus. This necessitates image differencing to obtain the light curve of the SN. Image subtraction was performed with HOTPANTS⁸, and the flux in each difference pair was determined via aperture photometry at the location of the SN. An example subtraction, which clearly shows flux from SN 2006gy after the reference image has been subtracted, is shown in Figure 1.

Despite observations extending more than two years past the date of discovery, SN 2006gy has not faded beyond the point of detectability with PAIRITEL. Consequently, all J , H , and K_s images of SN 2006gy con-

⁶ All dates in this paper are UT unless otherwise noted.

⁷ Following Smith et al. (2007), we adopt 2006 August 20 as the explosion date for SN 2006gy.

⁸ <http://www.astro.washington.edu/users/becker/hotpants.html>

tain some flux from the SN. We thus adopted the “NN2 method” of Barris et al. (2005) to determine the relative NIR flux changes of the SN. The NN2 method treats all images equally and does not require a template image with no light from the source of interest, SN 2006gy. It uses the subtraction of all $N(N - 1)$ pairs of images to mitigate against possible errors associated with the use of a single reference template image. The downside to the NN2 method is that it only produces the differential flux between each of the N epochs of observations. To convert these flux differences into magnitudes requires an absolute calibration, which must be obtained independently of the results from the NN2 method. Uncertainties in the individual subtractions were estimated by measuring the scatter in fake SNe inserted at locations having a surface brightness similar to that at SN 2006gy.

Early-time NIR observations of SN 2006gy (defined here as those made before SN 2006gy passed behind the Sun during 2007) show a remarkably flat light curve, as seen in Figure 2. To transform the relative-flux differences from the NN2 method to an absolute scale, we subtracted the archival Two Micron All Sky Survey (2MASS; Skrutskie et al. 2006) image from each of the images obtained on 2006 Nov. 13.24, 14.25, 15.38, and 16.37 to determine the J , H , and K_s magnitudes of the SN on these dates. The mean SN flux was then used to transform the relative flux from the NN2 method to the absolute flux of the 2MASS system (Cohen, Wheaton, & Megeath 2003). PAIRITEL uses the old 2MASS camera and telescope; hence, we do not expect any large systematic effects in the 2MASS subtractions. The final calibrated J , H , and K_s photometry is summarized in Table 1.

On 2006 Nov. 01, Ofek et al. (2007) obtained adaptive optics (AO) images in the J and K_s bands with the Palomar Hale (5 m) telescope, clearly resolving SN 2006gy from the host-galaxy nucleus, and measured its flux. In the K_s band our calibration and the Ofek et al. (2007) measurement agree to within 1σ , while the agreement in the J band is somewhat worse ($\sim 2\sigma$). Ofek et al. (2007) had only a single 2MASS star within the field of view of their AO images, whereas >100 2MASS stars were used to calibrate the PAIRITEL images; when coupled with the difficulty associated with photometry of AO images, this may explain the differences between the two measurements. We note that were we to adopt the Ofek et al. (2007) measurements as our calibration, there would be an overall systematic shift of our J and K_s light curves to brighter values, which in turn would lead to worse agreement between the NIR data and early-time optical spectra (see Figure 4). This suggests that our calibration method is sufficient. We note that the uncertainties in our photometry are dominated by the uncertainty in the calibration, which is ~ 0.03 mag in J , ~ 0.06 mag in H , and ~ 0.04 mag in K_s . This uncertainty is the same for all epochs, so a change in the calibration would lead to a systematic shift of the entire light curve.

As shown by Smith et al. (2008b), and subsequently confirmed by Agnoletto et al. (2009), the NIR evolution of SN 2006gy is very slow at late times. Given the relatively small change in flux, and the reduced signal-to-noise ratio following the fading of the SN, we were unable to recover reliable flux measurements from PAIRITEL data taken after 2007 Sep. Furthermore, unlike the case at early times, the SN had faded below the 2MASS detec-

TABLE 1
PAIRITEL OBSERVATIONS OF SN 2006GY

$t_{\text{mid}}^{\text{a}}$ (MJD)	J mag ^b (Vega)	H mag ^b (Vega)	K_s mag ^b (Vega)
54021.29	13.33 ± 0.04	13.05 ± 0.06	12.81 ± 0.05
54022.28	13.33 ± 0.04	13.08 ± 0.09	12.83 ± 0.05
54024.30	13.29 ± 0.04	13.03 ± 0.06	12.84 ± 0.06
54027.22	13.32 ± 0.04	13.03 ± 0.06	12.78 ± 0.04
54028.23	13.26 ± 0.04	13.03 ± 0.06	12.81 ± 0.05
54029.46	13.27 ± 0.03	13.02 ± 0.06	12.81 ± 0.06
54030.47	13.27 ± 0.04	13.01 ± 0.06	12.79 ± 0.04
54031.45	13.27 ± 0.04	13.01 ± 0.06	12.81 ± 0.05
54035.26	13.25 ± 0.04	13.02 ± 0.06	12.78 ± 0.04
54036.25	13.21 ± 0.05	13.00 ± 0.06	12.77 ± 0.04
54037.28	13.25 ± 0.03	13.02 ± 0.06	12.76 ± 0.04
54039.28	13.23 ± 0.04	13.01 ± 0.06	12.77 ± 0.04
54040.29	13.25 ± 0.04	13.01 ± 0.06	12.77 ± 0.05
54041.31	13.29 ± 0.04	13.01 ± 0.06	12.78 ± 0.04
54042.32	13.22 ± 0.05	13.03 ± 0.08	12.79 ± 0.09
54044.27	13.26 ± 0.04	13.00 ± 0.06	12.74 ± 0.04
54045.27	13.28 ± 0.05	13.00 ± 0.06	12.79 ± 0.05
54046.25	13.33 ± 0.04	13.02 ± 0.07	12.80 ± 0.05
54047.25	13.26 ± 0.03	12.99 ± 0.06	12.76 ± 0.05
54048.23	13.29 ± 0.04	13.02 ± 0.06	12.74 ± 0.05
54049.23	13.27 ± 0.04	13.01 ± 0.06	12.78 ± 0.05
54050.27	13.25 ± 0.03	13.00 ± 0.06	12.78 ± 0.04
54051.31	13.25 ± 0.04	13.00 ± 0.06	12.76 ± 0.04
54052.25	13.24 ± 0.04	13.00 ± 0.06	12.77 ± 0.04
54053.26	13.25 ± 0.03	13.01 ± 0.06	12.76 ± 0.04
54054.38	13.27 ± 0.04	13.01 ± 0.06	12.76 ± 0.04
54055.38	13.28 ± 0.04	13.01 ± 0.06	12.77 ± 0.04
54058.18	13.27 ± 0.03	13.00 ± 0.06	12.75 ± 0.04
54059.19	13.24 ± 0.04	13.01 ± 0.06	12.74 ± 0.05
54060.22	13.27 ± 0.03	13.01 ± 0.06	12.79 ± 0.04
54061.21	13.24 ± 0.04	13.01 ± 0.06	12.75 ± 0.05
54063.24	13.28 ± 0.04	13.00 ± 0.06	12.74 ± 0.05
54064.24	13.30 ± 0.04	13.01 ± 0.06	12.76 ± 0.04
54065.24	13.24 ± 0.07	13.08 ± 0.11	12.83 ± 0.19
54066.25	13.31 ± 0.04	13.01 ± 0.06	12.76 ± 0.05
54069.15	13.27 ± 0.04	13.04 ± 0.06	12.82 ± 0.05
54070.13	13.31 ± 0.04	13.02 ± 0.06	12.77 ± 0.04
54071.15	13.31 ± 0.05	13.02 ± 0.06	12.83 ± 0.05
54072.13	13.28 ± 0.04	13.01 ± 0.06	12.77 ± 0.04
54074.09	13.31 ± 0.04	13.03 ± 0.06	12.82 ± 0.05
54075.13	13.31 ± 0.04	13.01 ± 0.06	12.77 ± 0.05
54076.12	13.37 ± 0.04	13.02 ± 0.06	12.79 ± 0.04
54077.12	13.37 ± 0.04	13.02 ± 0.06	12.80 ± 0.04
54079.18	13.34 ± 0.05	13.03 ± 0.06	12.80 ± 0.05
54080.18	13.41 ± 0.05	13.06 ± 0.06	12.80 ± 0.04
54081.17	13.40 ± 0.04	12.98 ± 0.06	12.82 ± 0.05
54082.15	13.32 ± 0.07	13.07 ± 0.07	12.79 ± 0.05
54083.16	13.36 ± 0.09	13.00 ± 0.06	12.75 ± 0.05
54084.14	13.39 ± 0.05	13.05 ± 0.06	12.84 ± 0.08
54085.13	13.40 ± 0.05	13.08 ± 0.07	12.84 ± 0.05
54086.13	13.48 ± 0.06	13.06 ± 0.07	12.88 ± 0.06
54090.08	13.42 ± 0.04	13.11 ± 0.07	12.88 ± 0.05
54091.08	13.59 ± 0.09	13.11 ± 0.07	12.93 ± 0.05
54092.29	13.51 ± 0.11	13.06 ± 0.06	12.90 ± 0.07
54094.12	13.68 ± 0.11	13.12 ± 0.07	12.90 ± 0.05
54095.12	13.66 ± 0.11	13.13 ± 0.07	13.00 ± 0.16
54100.14	13.79 ± 0.08	13.15 ± 0.07	13.03 ± 0.13
54101.15	13.81 ± 0.07	13.16 ± 0.07	13.16 ± 0.14

^aMidpoint between the first and last exposures in a single stacked image.

^bObserved value; not corrected for Galactic extinction.

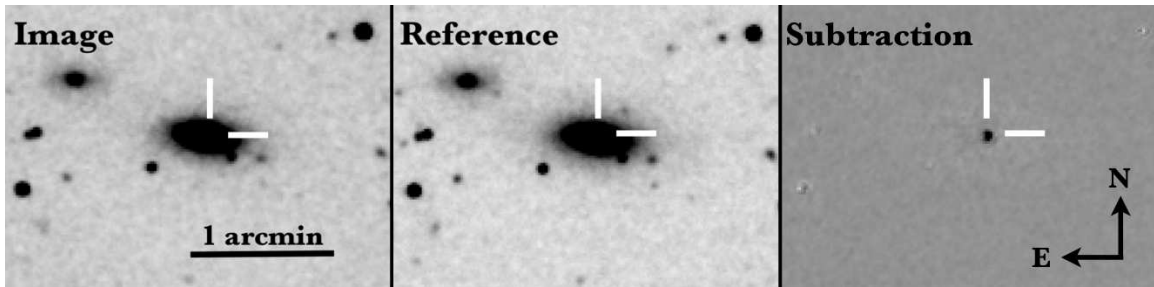


FIG. 1.— Example subtraction of PAIRITEL NIR images of SN 2006gy, which have all been registered to the same coordinate frame. Each image is $\sim 2' \times 3'$ in size. *Left*: PAIRITEL K_s -band image taken on 2006 Nov. 15. *Middle*: PAIRITEL K_s -band image taken on 2007 Jan. 01. *Right*: Image (left panel) minus reference (middle panel) subtraction image. The image subtraction was performed with HOTPANTS, and SN 2006gy is clearly visible in the difference image as a bright point source near the galaxy nucleus.

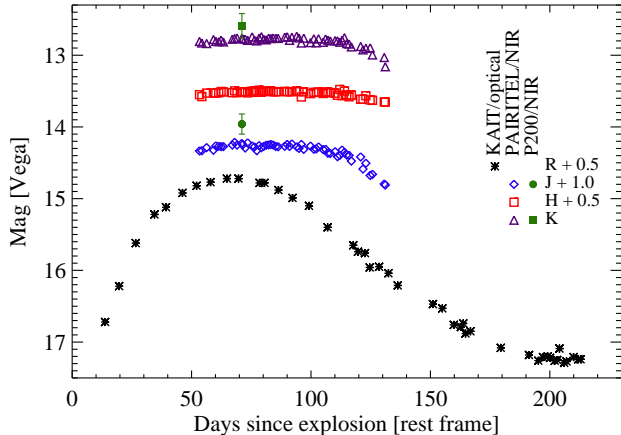


FIG. 2.— Early-time photometric evolution of SN 2006gy. Unfiltered KAIT (roughly R band) observations are taken from Smith et al. (2007). PAIRITEL J , H , and K_s observations are from this work. We also show the Palomar AO photometry from Ofek et al. (2007). The data have not been corrected for extinction in the host or the Galaxy. The NIR evolution is remarkably flat, with the $R - K$ color increasing steadily after day ~ 70 . This behavior is consistent with a cooling blackbody (see text).

tion limit, which means that the late-time subtractions relative to the 2MASS template image do not yield meaningful results despite the fact that at $K_s \approx 15$ the SN is well above the PAIRITEL detection limit. In principle, if deep PAIRITEL images are obtained after SN 2006gy fades well beyond the detection limit, it should be possible to recover the late-time NIR light curve using template images that contain little or no light from the SN.

We also observed SN 2006gy on 2008 Aug. 25 with the Near-Infrared Camera 2 (NIRC2) using the laser guide star (LGS) AO system (Wizinowich et al. 2006) on the 10-m Keck II telescope in Hawaii. We have reduced the LGS AO images presented by Smith et al. (2008b) from days 398 and 461⁹ and derive revised values for the K' -band magnitudes of SN 2006gy, as summarized in Table 2.¹⁰ The uncertainty on these measurements is large ($\gtrsim 0.17$ mag), and is dominated by the uncertainty in the single calibration star within the field of view. We also

⁹ Note that Smith et al. (2008b) refer to these epochs as day 405 and 468, which is the elapsed time in the observed frame. All epochs in the present work are labelled in terms of the elapsed time in the rest frame.

¹⁰ Late-time Keck AO observations were all made in the K' band. The uncertainty associated with the transformation between K' and K_s is small compared to the absolute calibration uncertainty; hence, for the late-time AO images $K' \approx K_s$.

TABLE 2
KECK AO OBSERVATIONS OF SN 2006GY

date (UT)	epoch ^a (day)	Filter	mag ^b (Vega)
2007 Sep. 29	398	K'	14.91 ± 0.17
2007 Dec. 02	461	H	16.8 ± 0.3
2007 Dec. 02	461	K'	15.02 ± 0.17
2008 Aug. 25	723	K'	15.59 ± 0.21

^aRest-frame days from the adopted explosion date, 2006 Aug. 20 (Smith et al. 2007).

^bObserved value; not corrected for Galactic extinction.

present the first measurement of the H -band flux from the AO images taken on 2007 Dec. 2. To obtain this H -band measurement, despite a lack of 2MASS stars in the field, we measured the $H - K'$ color of SN 2006gy relative to the $H - K'$ color of the host galaxy, and calibrated this against the $H - K_s$ color of the galaxy in the archival 2MASS images. The large uncertainty for this measurement reflects the accuracy with which we can determine the color of the galaxy from the 2MASS images.

As part of a *Hubble Space Telescope* (HST) snapshot survey (GO-10877; PI Li), SN 2006gy was observed with the Wide Field Planetary Camera 2 (WFPC2; Holtzman et al. 1995a) using the $F450W$, $F555W$, $F675W$, and $F814W$ filters on 2008 Nov. 22. The data were reduced in the standard fashion using **multidrizzle** (Koekemoer et al. 2002). NGC 1260 and SN 2006gy were located at the center of the PC chip of WFPC2, which has a native pixel scale of $0.0455'' \text{ pixel}^{-1}$. We follow the recipe of Dolphin (2000) to do charge-transfer efficiency correction and photometric reduction of the WFPC2 images. Our measurements of the SN 2006gy magnitudes are summarized in Table 3. A false-color image of this detection is shown in Figure 3.

3. DISCUSSION

3.1. Early-Time NIR Observations

While the early-time evolution of SN 2006gy is remarkably flat in the NIR (see Figure 2), we find that these measurements are consistent with radiation from a cooling blackbody. From blackbody fits to optical spectra, Smith et al. (2010) find that the temperature of SN 2006gy monotonically cools after day ~ 50 , roughly two weeks before optical maximum, until day ~ 165 , where the temperature levels off at ~ 6300 K. In the top panel of Figure 4 we show the evolution of the SED of SN 2006gy for three epochs (day 58, 107, and 133) during our early-time NIR observations. These three

TABLE 3
HST DAY 810 OBSERVATIONS OF SN 2006GY

Filter	$\lambda_{\text{cent}}^{\text{a}}$ (Å)	$\Delta\lambda^{\text{b}}$ (Å)	mag^{c} (Vega)	Flux^{d} (μJy)
<i>F450W</i>	4519	957	22.16 ± 0.03	5.97 ± 0.18
<i>F555W</i>	5397	1226	21.51 ± 0.02	9.31 ± 0.19
<i>F675W</i>	6697	866	21.07 ± 0.03	11.29 ± 0.34
<i>F814W</i>	7924	1500	20.91 ± 0.04	10.80 ± 0.43

^aCentral wavelength of the filter, based on WFPC2 calibrations presented in Table 8 of Holtzman et al. (1995b).

^bFilter width, based on WFPC2 calibrations presented in Table 8 of Holtzman et al. (1995b).

^cObserved value; not corrected for Galactic extinction.

^dObserved flux using the photometric calibrations presented in Table 9 of Holtzman et al. (1995b).

epochs were chosen as a representative sample covering the full range of our early NIR observations. The evolution of the SED is gradual; the three epochs shown in Figure 4 are not more or less statistically significant, in terms of the observed NIR excess (see below), than other epochs from similar times. For each epoch we show the single-component blackbody spectrum, after adopting the temperature from Smith et al. (2010) and normalizing the spectra to the photometric measurements from Smith et al. (2007). Their photometric observations come from a series of unfiltered observations taken with the Katzman Automatic Imaging Telescope (KAIT; Filippenko et al. 2001), which are best matched by the *R* band (Riess et al. 1999; Li et al. 2003). However, the scatter in the transformation between KAIT unfiltered and *R* can be quite large (Ganeshalingam 2009), so we adopt a 0.1 mag uncertainty for the calibration of the blackbody spectra. We also show the NIR flux during these epochs, determined from the absolute calibration of the 2MASS system (Cohen, Wheaton, & Megeath 2003). This shows excellent agreement with an extrapolation of the early-time spectra of SN 2006gy (Smith et al. 2010). Between day ~ 55 –135 roughly 2–4% of the bolometric luminosity of SN 2006gy was emitted in the NIR.

In the lower panel of Figure 4 we show the fractional excess of the photometric observations relative to the single-component blackbodies (note that by definition the *R*-band excess is set to zero). For clarity we do not show the uncertainties associated with the excess, but after accounting for the large uncertainty in the *R*-band calibration, each point is within $\sim 1\sigma$ of zero excess. Nevertheless, there is an apparent trend that the excess is growing in the *H* and *K_s* bands as a function of time. The trend may be indicative of radiation from warm dust (see below), though we note that this effect would be small. If this trend toward a NIR excess is created by the same source as the late-time NIR excess, we would expect a *K_s*-band excess of ~ 0.17 mag, which is comparable to the combined uncertainty from the blackbody calibration and photometric measurements.

3.2. Late-Time NIR Observations

With data obtained more than a year after explosion, Smith et al. (2008b) discovered a significant NIR excess from SN 2006gy. Our NIR observations taken 723 days after explosion show that the *K'*-band flux from SN 2006gy has only faded by a factor of ~ 2 over the course of the previous year. We cannot determine the total IR luminosity at late times, because our NIR data

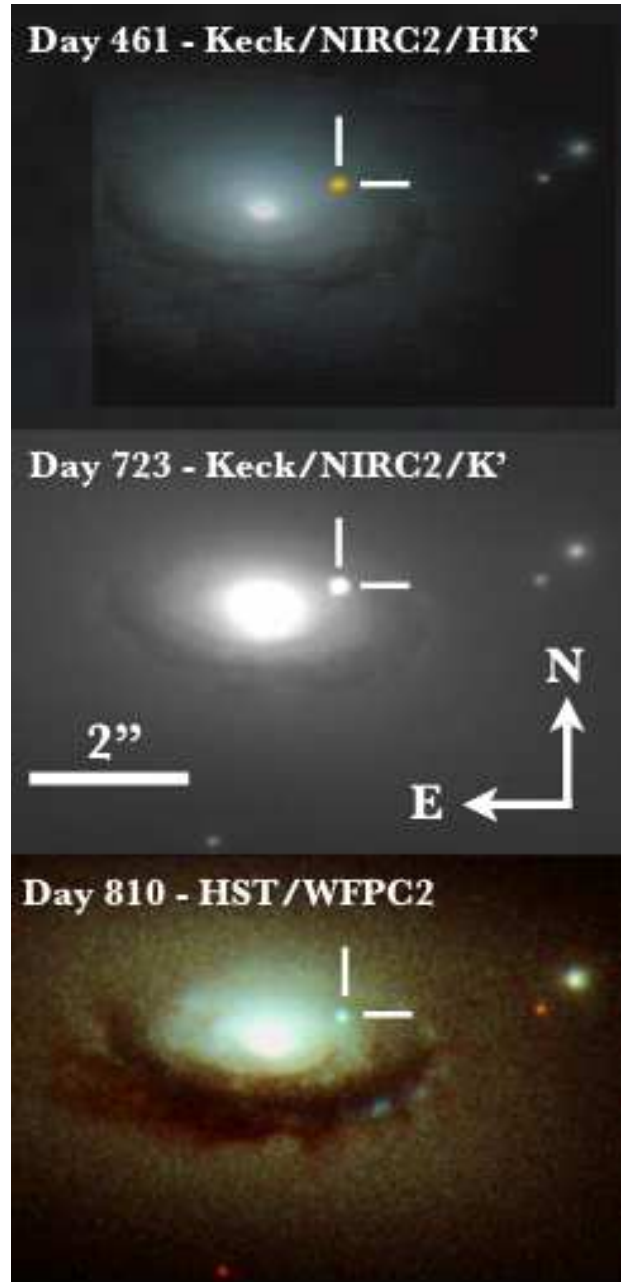


FIG. 3.— Late-time optical and NIR images of SN 2006gy. *Top*: Keck AO *H* and *K'* false-color image from Smith et al. (2008b). The SN is clearly red in the NIR. Note that the field of view for this image is slightly smaller than that of the others. *Middle*: Keck AO *K'* image of SN 2006gy taken on day 723. The SN is still clearly visible in the NIR, and has shown little change since observations taken around day 400. *Bottom*: *HST* WFPC2 false-color image including the four filters in which we detect SN 2006gy: *F450W* (corresponding to blue), *F555W*, *F675W*, and *F814W* (corresponding to red). The SN is clearly blue in the optical compared to the light from the surrounding stars.

do not cover the peak of the SED. Furthermore, as first noted by Smith et al. (2008b), the very red *H* – *K'* color at late times indicates that the IR emission likely peaks in the mid-IR. To place a lower limit on the NIR luminosity we assume that the SED peaks in the *K'* band. Following this assumption, the NIR excess constitutes a slowly varying luminosity of $\gtrsim 2 \times 10^8 L_{\odot}$ for > 1 yr.

The most likely explanation for this large luminosity

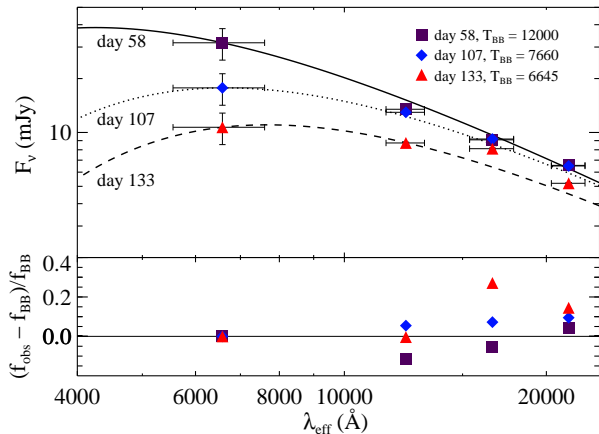


FIG. 4.— SED evolution of SN 2006gy at early times showing a possible trend toward a growing IR excess above a cooling blackbody. *Top*: the solid, dotted, and dashed lines show a single-component blackbody spectrum, normalized to unfiltered observations from Smith et al. (2007), on days 58, 107, and 133, respectively. *Bottom*: the fractional excess emission in J , H , and K_s , relative to the blackbody model. For clarity we do not include the uncertainties in these measurements, which are large and dominated by the uncertainty in the transformation between unfiltered data and the R band (see text). Each point is within $\sim 1\sigma$ of showing no excess; however, the NIR excess does appear to grow with time.

in the NIR is warm dust. The observed $H - K'$ color from day 436 corresponds to a temperature of ~ 1000 K, assuming a single-temperature blackbody. If the dust is radiating as a single blackbody with $T_{\text{peak}} = 1000$ K, this would increase the above luminosity to $\gtrsim 3 \times 10^8 L_{\odot}$. We note that our NIR observations are only sensitive to the warmest dust; it is possible that cooler dust with $T \approx 600$ K¹¹ could dominate the IR emission, in which case the luminosity could be significantly higher than the values quoted above.

The location of this dust, and whether it is newly formed or pre-existing at the time of the SN explosion, remain to be determined. The dust-cooling time is short, meaning that a prolonged heat source is needed to explain the extended excess. We consider four possibilities for heating the dust: (i) radioactive heating from ^{56}Co decay, (ii) collisional excitation of pre-existing dust, (iii) heating via radiation from circumstellar interaction, and (iv) a late-time IR dust echo, where pre-existing dust is heated by the radiation produced while the SN was near its optical peak.

3.2.1. Radioactive Heating from ^{56}Co

Smith et al. (2008b) noted that the observed K' -band decay between 2007 September and 2007 December could be explained with radioactive heating from a minimum of $2.5 M_{\odot}$ of ^{56}Ni , if a sufficient amount of dust formed in order to move the luminosity into the NIR (though they favored another interpretation; see below). We show the bolometric evolution of SN 2006gy through the first ~ 800 days post explosion, including both optical and NIR detections, in Figure 5. From Equation 19 of Nadyozhin (1994), and the fact that the luminosity from ^{56}Co de-

cay dominates over ^{56}Ni decay at times $\gtrsim 2$ weeks after explosion, we arrive at the following expression for the radioactivity-powered luminosity of a SN, assuming 100% trapping of gamma-rays:

$$L_{^{56}\text{Co}} = 1.45 \times 10^{43} \exp^{-t/(111.3 \text{ d})} M_{\text{Ni}}/M_{\odot} \text{ erg s}^{-1}, \quad (1)$$

where t is the time since SN explosion in days, and M_{Ni} is the total mass of ^{56}Ni produced. Using Equation 1 we also show in Figure 5 the expected light curve from $2.5 M_{\odot}$ of ^{56}Ni at times > 400 days. The early-time measurements (< 250 days) come from Smith et al. (2010). The optical measurement near day 400 comes from photometric measurements by Kawabata et al. (2009), while the optical luminosity on day 810 comes from a direct integration of our *HST* observations (see § 3.3.1). The three late-time NIR luminosities represent lower limits based on the measured K' -band flux (see above, § 3.2). The decay rate of ^{56}Co , $0.98 \text{ mag } (100 \text{ day})^{-1}$, is much faster than the observed decay of the K' flux from SN 2006gy, $\sim 0.2 \text{ mag } (100 \text{ day})^{-1}$. The late-time NIR excess declines at a rate that is too slow to be explained by ^{56}Co heating alone.

The PISN model of Nomoto et al. (2007), which provided good agreement with the early-time light curve of SN 2006gy after an artificial reduction of the total ejecta mass from their evolutionary calculation, was able to reproduce the late-time NIR luminosity observed by Smith et al. (2008b). This model required less than 100% efficiency in the conversion of gamma-rays (from radioactive decay) to optical/NIR emission, which means that the light curve should decay *faster* than $0.98 \text{ mag } (100 \text{ day})^{-1}$. The possibility of a PISN was first invoked to explain the large peak luminosity of SN 2006gy (Ofek et al. 2007; Smith et al. 2007). This scenario would have required the production of $\gtrsim 10 M_{\odot}$ of ^{56}Ni , which in turn would produce a large late-time luminosity that decays at the rate of ^{56}Co . The late-time NIR luminosity is not accounted for in either the general PISN models or the artificial model of Nomoto et al. (2007); it therefore provides a serious challenge to the PISN hypothesis.¹²

3.2.2. Collisional Heating of the Dust

Another possibility is that the dust existed prior to the SN explosion, at large distances from the explosion site, and was heated via collisions with the expanding material in the expanding blast wave. The intense UV/optical output from a SN at its peak vaporizes any dust in the vicinity of the SN (Dwek 1983). This radiation near peak creates a dust-free cavity into which the SN ejecta may expand at early times; however, the ejecta blast wave will eventually reach the edge of the dust-free cavity, at which point collisional excitations of the dust may generate NIR emission.

The large peak luminosity of SN 2006gy, $8 \times 10^{10} L_{\odot}$ (Smith et al. 2010), provides significant challenges to this collisional heating scenario. Dwek (1983) shows that the radius of the dust-free cavity can be determined from

¹¹ Smith et al. (2008b) show that the combination of the peak luminosity and distance to the dust suggest an equilibrium temperature around 600 K.

¹² The pulsational pair-instability model of Woosley, Blinnikov, & Heger (2007) has not, however, been excluded; see also Smith et al. (2010).

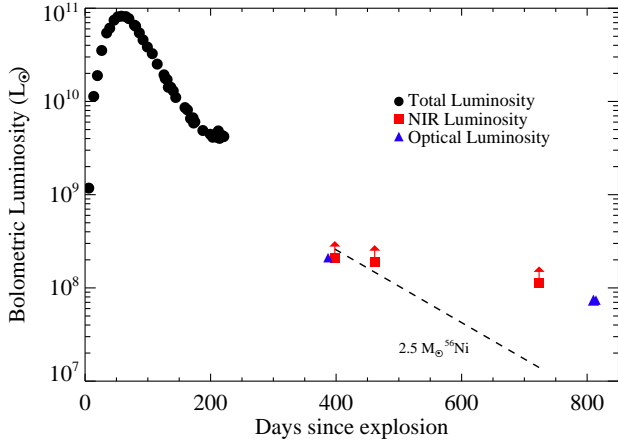


FIG. 5.— Evolution of the bolometric luminosity of SN 2006gy during the first 800 days after explosion. Optical data are shown as black circles, and NIR data are red squares. Early-time data (< 250 days) are from Smith et al. (2010). The optical detection near day 400 is from Kawabata et al. (2009). All other data are from this work. NIR measurements are only lower limits to the total IR luminosity, because our observations do not sample redward of 2.2 μm (see text). The dashed line shows the expected decline if the luminosity were powered by 2.5 M_{\odot} of ^{56}Ni . The flat nature of the light curve indicates that radioactivity is not the primary energy source for the late-time emission.

the peak luminosity and the dust vaporization temperature, assuming the grain emissivity Q_v is proportional to $(\lambda/\lambda_0)^{-1}$:

$$R_1(\text{pc}) = 23 \left[\frac{\bar{Q}_v L_0 (L_{\odot})}{\lambda_0 (\mu\text{m}) T_v^5} \right]^{0.5}, \quad (2)$$

where R_1 is the radius of the dust-free cavity, \bar{Q}_v is the mean grain emissivity, L_0 is the peak luminosity, and T_v is the dust vaporization temperature. Following Dwek (1983), if we assume $\bar{Q}_v = 1$ and that $\lambda_0 = 0.2 \mu\text{m}$, we find that $R_1 \approx 1.4 \times 10^{18}$ cm, for a vaporization temperature $T_v \approx 1000$ K. If the absorption coefficient is instead proportional to λ^{-2} , then the cavity becomes even larger. Based on the observed width of the $\text{H}\alpha$ line from SN 2006gy, Smith et al. (2007) estimate the speed of the blast wave to be 4000 km s^{-1} , which would mean that this material would take ~ 112 yr to reach the edge of the dust-free cavity. Even if there are ejecta traveling at more typical SN velocities of $10,000 \text{ km s}^{-1}$, it would take over 45 yr for this material to reach the edge of the dust-free cavity. Given that the NIR excess is present ~ 1 yr following explosion, and that the SN ejecta could not reach the dust in such a short time, collisional heating of dust by SN ejecta cannot explain the observed NIR excess. Large grains will persist at smaller radii than smaller grains according to Equation 2, since the size of the dust-free cavity is $\propto \lambda_0^{-0.5}$, while the grain size, $a = \lambda_0/2\pi$. The existence of grains at $R_1 \approx V_{\text{SN}} t_{\text{SN}} = 4000 \text{ km s}^{-1} \times 1 \text{ yr} = 1.26 \times 10^{16}$ cm, and thus possibly explain the NIR excess seen 1 yr after explosion, would require dust particles a factor $\sim 10^4$ larger than those assumed above, roughly corresponding to ~ 1 mm size grains. Such large grains are rare and are inefficient radiators in the NIR (Spitzer 1978); therefore, they are unlikely to explain the observed NIR excess.

3.2.3. Newly Formed Dust

The emission features that arise in SNe IIn, as in SN 2006gy, originate from the interaction of the SN ejecta with a dense CSM. Shocked gas, located between the forward shock which is plowing into the CSM and a reverse shock of the SN ejecta, can cool, and if the density is large enough, it may form new dust grains. The cooling time for such dust is short, and can be estimated in the following manner: $\tau_{\text{cool}} \approx E/L$ where E is the thermal energy of a grain and L is the grain luminosity. We estimate the thermal energy as $Nk_B T_{\text{dust}}$, where N is the total number of particles in a grain and k_B is the Boltzmann constant. We assume the grains radiate as a blackbody: $L = 4\pi a^2 \sigma T_{\text{dust}}^4$, where a is the typical grain size and σ is the Stefan-Boltzmann constant. For graphite grains of size $a \approx 1 \mu\text{m}$, and $\rho \approx 3 \text{ g cm}^{-3}$, we have $N \approx 10^{12}$, meaning $\tau_{\text{cool}} < 1$ s. Furthermore, theoretical calculations by Draine & Li (2001) show that the cooling time for PAH and silicate grains at $T \approx 1000$ K is $\lesssim 10$ s, for grains of all sizes. Nevertheless, a persistent heat source can generate an extended period of NIR emission. The physical conditions for post-shock dust formation are not necessarily easy to produce: strongly interacting SNe are often X-ray sources, which could prevent the formation of new dust grains in the post-shock gas. Evidence for the formation of dust in the post-shock region has been found for a few SNe, however, including SN 1998S (Pozzo et al. 2004), SN 2006jc (Smith, Foley, & Filippenko 2008), and SN 2005ip (Smith et al. 2009; Fox et al. 2009). This newly formed dust is then heated by the energy from the shock as it continues to propagate into the CSM, which gives rise to the prolonged NIR excess.

This scenario is difficult to reconcile with the case of SN 2006gy, however. Spectra taken around day 200 show a decline in the luminosity of the $\text{H}\alpha$ emission line, which indicates a reduction in the CSM interaction at this time (Smith et al. 2010). Furthermore, as detailed by Smith et al. (2008b), the lack of X-ray, $\text{H}\alpha$, and radio emission a little more than a year after the SN explosion implies that the observed NIR luminosity cannot be explained by shock-heated dust. In fact, the radio nondetection of SN 2006gy continues through day 638 (Bietenholz & Bartel 2008). Kawabata et al. (2009) do claim the detection of very weak $\text{H}\alpha$ emission from SN 2006gy on day 394, but the inferred luminosity of $\sim 10^{39} \text{ erg s}^{-1}$ is nearly three orders of magnitude lower than the observed NIR luminosity at this time. Kawabata et al. (2009) also claim an R -band detection of 19.4 mag on day 394 (though we note that Smith et al. 2008b report an upper limit of $R > 20$ mag, and Agnoletto et al. 2009 give an upper limit of $R > 20.3$ mag, at a similar epoch), which would constitute an optical luminosity similar to that observed in the NIR. The source of this optical luminosity could potentially be the heat source for newly formed dust at day ~ 400 , though it cannot explain the similar NIR luminosity seen on day 723. While SN 2006gy was detected in the optical at > 800 days to have a luminosity similar to that seen in the NIR, the very blue nature of optical data suggests that it is a scattered-light echo (see Section 3.3) of UV/optical emission from the SN peak. The light echo must originate *outside* the dust-forming region and therefore can-

not heat the dust. While we cannot strongly rule out dust formation in the post-shock region of SN 2006gy, it is implausible to explain the late-time NIR luminosity via new dust, because there are no signs of a heating source that lasts for > 1 yr.

3.2.4. NIR Dust Echo

Perhaps the most natural explanation for the late-time NIR excess is a dust-heated echo, as first discussed by Smith et al. (2008b). In this scenario, the IR emission comes from dust near the explosion site which is heated by the early-time UV/optical emission from the SN. IR echo models by Dwek (1983) predict a fast rise (of order the rise time in the optical of the SN) in the IR, followed by an extended plateau (lasting > 1 yr; see below) before the IR luminosity follows a rapid decline (where the IR flux declines as e^{-t}/t). The extended plateau from an IR echo matches the qualitative behavior of SN 2006gy, which exhibits a very slow decline in the NIR: only a factor of ~ 2 in flux over the course of ~ 1 yr.

Assuming isotropic optical emission from the SN, the plateau occurs because the hottest dust, which exists right at the edge of the dust-free cavity described above, dominates the emission. According to the view of a distant observer, the emitting volume is a series of paraboloid light fronts that expand throughout the dust-free cavity as shown in Figure 6 (see also Figure 1 of Dwek 1983). As a paraboloid expands it continually heats dust at R_1 , which is what gives rise to the plateau in the light curve. After a time $\sim 2R_1/c$, the vertex of a given paraboloid will reach the back edge of the cavity and will no longer be heating dust at R_1 . Emission from the dust will be dominated by the UV/optical radiation produced by the SN at peak, and once this radiation sweeps past the back edge of the cavity the IR luminosity begins to rapidly decline. Therefore, if we know the duration of the plateau phase we can determine the size of the dust-free cavity. Constraints on the cavity size can be determined by assuming that the echo starts at our first K' observation on day 398 and ends on our last observation on day 723. In this case we find that $R_1 \approx 4 \times 10^{17}$ cm; however, it would be contrived if our observations were to perfectly bookend the plateau phase of the echo: the echo almost certainly started prior to day 398 and continued beyond day 723. In fact, the model predicts that the echo should start well before day ~ 400 . There is mild evidence for a NIR echo as early as day ~ 130 : the H -band and K_s -band flux is (respectively) $\sim 2\sigma$ and $\sim 1\sigma$ greater than their expected values based on an extrapolation of optical spectra (see Figure 2). If we instead assume that the slight NIR excess seen at day ~ 130 (see Figure 2) is the rise of an IR echo, then we find that $R_1 \approx 8 \times 10^{17}$ cm, which shows reasonable agreement with the value we calculated for the dust-free cavity in § 3.2.2, $R_1 \approx 1.4 \times 10^{18}$ cm, considering the uncertainties in the dust temperature and the likelihood that the plateau extends beyond day 723.

Our NIR observations are only sensitive to the warmest dust, but if we assume that the NIR luminosity peaks in the K' band, then a lower limit to the total energy emitted in the IR is $E_{\text{IR}} \approx 2 \times 10^8 L_{\odot} \times 600$ days, or $\gtrsim 4 \times 10^{49}$ erg. This is comparable to the canonical optical output of a normal SN II. Typically, this would pose a significant problem for the IR echo hypothesis, as it

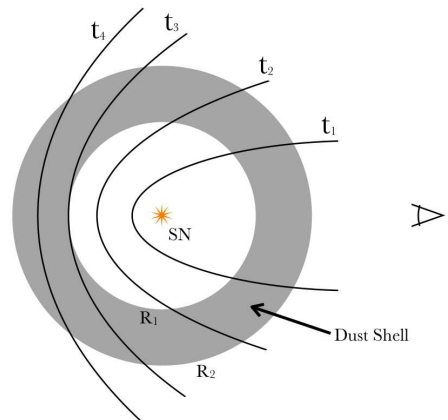


FIG. 6.— Schematic diagram showing the evolution of an IR echo arising from a circumstellar dust shell, shown in the shaded area. The large luminosity from the SN vaporizes a dust-free cavity out to radius R_1 . At early times the dust-emitting volume is small, shown as the area interior to the parabola marked t_1 , as the radiated light from other portions of the shell has not had sufficient time to reach the observer. As time increases, so does the emitting volume, to the area within t_2 , then t_3 , etc. The echo luminosity is dominated by the warmest dust at $\sim R_1$. As the light parabola sweeps through the shell, new emission from dust at $\sim R_1$ continually becomes observable, leading to a plateau in the NIR light curve. The plateau continues until a time $t_3 \approx 2R_1/c$, at which point the parabola has swept past the inner edge of the shell. Additional emission continues to be observable (t_4); however, this is from more distant, cooler dust and as a result the IR echo falls off the plateau and begins to decline.

would require of order unity of the original optical radiation from the SN to be absorbed and reradiated in the NIR. Indeed, this is precisely the argument used by Fox et al. (2009) to argue against the light-echo hypothesis for SN 2005ip. In the case of SN 2006gy this is not a problem, however, because the NIR emission falls well within the available energy budget to heat the dust. After applying a bolometric correction, Smith et al. (2010) find that $\sim 2.5 \times 10^{51}$ erg were emitted by SN 2006gy during the first ~ 220 days of the light-curve evolution, which means that less than 2% of this energy has been absorbed and reradiated by the dust. This value is comparable to those found by Dwek (1983) for SNe 1979C and 1980K.

If we assume that the dust radiates as a blackbody, we can estimate the optical depth of the dust shell as $\tau \approx E_{\text{IR}}/(E + E_{\text{IR}}) \approx 0.016$. We note that like E_{IR} above, this value constitutes a lower limit for τ . Even if the NIR luminosity is a factor of 10 larger than our lower limits, this would imply $\tau \approx 0.1$, which corresponds to an optical extinction of $A_V = 1.086\tau \approx 0.1$ mag. This is far less than the total observed extinction from the host, $A_{V,\text{host}} \approx 1.67$ mag (Smith et al. 2007), suggesting that the dusty shell responsible for the IR echo cannot produce all of the non-Galactic reddening observed toward SN 2006gy. That there is a considerable amount of dust along the line of sight, which is not in the CSM of SN 2006gy, should not come as a surprise given that there is a prominent dust lane in NGC 1260 (see Figure 3).

With this information in hand, it is now possible to estimate the total dust mass of the shell that creates the NIR echo. According to Dwek (1983) for a dust shell with density $n_d \propto r^{-2}$,

$$M_d = 4\pi \left(\frac{4\rho_{gr}a}{3\bar{Q}_\nu} \right) \tau_d \times \frac{R_1 R_2^2}{R_2 - R_1}, \quad (3)$$

where M_d is the total dust mass in the shell, ρ_{gr} is the grain density, a is the grain radius, τ_d is the optical depth, \bar{Q}_ν is the mean absorption efficiency, and R_1 and R_2 are the inner and outer radii of the dust shell, respectively. Above we estimate the inner radius of the dust shell to be $\sim 8 \times 10^{17}$ cm. The value of the outer radius can be deciphered from the decay of the NIR light curve following the plateau. As we have not yet observed the NIR decay, we adopt an outer radius of $2R_1$, which provides a *lower limit* to the dust mass in the shell. Finally, we follow the same assumptions as Dwek (1983) about the dust properties: $\rho_{gr} = 3 \text{ g cm}^{-3}$, $a = 0.1 \mu\text{m}$, and $\bar{Q}_\nu = 1$. With these assumptions we find a total dust mass of $M_d \approx 0.1 M_\odot$. Assuming a typical value for the dust-to-gas ratio, 1:100, the total mass of the circumstellar shell is $\sim 10 M_\odot$. This value shows good agreement with the initial estimate of 5–10 M_\odot from Smith et al. (2008b), which was based only on observations taken between 400 and 461 days after explosion. We note that $\sim 10 M_\odot$ constitutes a lower limit to the total mass of the shell, because the actual value of the duration of the plateau and E_{IR} could potentially be much larger than the values we adopted above.

At a distance of $\sim 10^{18}$ cm from the SN explosion site, it is not immediately evident whether the dust giving rise to the NIR echo is part of the progenitor’s CSM or the local interstellar medium (ISM). Smith et al. (2008b) argue that the large dust mass needed at $\sim 10^{18}$ cm could be explained if the progenitor passed through a phase of eruptive mass loss ~ 1000 – 1500 yr prior to explosion, in an event similar to observed outbursts from η Car. Pre-existing dust in the walls of a giant H II region, where a massive star like the progenitor of SN 2006gy might have lived, cannot account for the IR echo because at typical distances of ~ 10 pc or more from the SN, the dust would be far too cold to reproduce the NIR excess.

3.3. Observed Color Evolution from HST Observations

Chevalier (1986) predicts that any SN with an IR echo due to pre-existing CSM dust should also show a faint scattered-light echo in the optical as well. He shows that this dust can lead to optical emission characterized by a $\lambda^{-\alpha}$ scattering law, where α is some value between 1 and 2. More than a year after explosion SN 2006gy had faded rapidly in the optical (Smith et al. 2008b; Agnoletto et al. 2009; Kawabata et al. 2009). Therefore, we obtained *HST* images to search for a possible late-time scattered-light echo.

Our optical detection on day 810 shows a significant change in the optical decline rate of SN 2006gy. During the interval 200–400 days the SN faded by $\gtrsim 3$ mag in the optical (Smith et al. 2008b), whereas the decline over days 400–810 was only ~ 1 mag. In addition to this reduced rate of decline, the SN underwent significant color evolution. Assuming that *F555W* and *F814W* approximate the *V* and *I* bands, respectively, we find that $V - I = 0.60$ mag on day 810. By contrast, with a 12,000 K color temperature at peak (Smith et al. 2010), the observed color of SN 2006gy would have been $V - I \approx 1.01$ mag. Thus, the spectrum on day 810 is

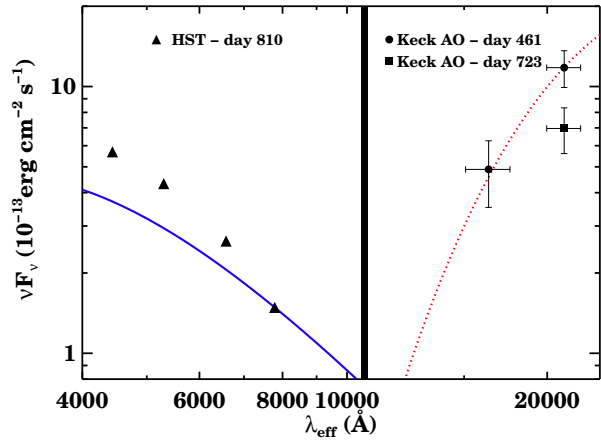


FIG. 7.— Late-time SED of SN 2006gy showing evidence for two distinct emission components. We show the flux in the optical (*HST*, day 810) and NIR (Keck AO, days 461 and 723), corrected for host-galaxy and Milky Way reddening. The vertical solid line is to remind the reader that optical and NIR observations were not taken simultaneously. The solid blue line shows a 12,000 K blackbody, normalized to the *F814W* detection. The red dotted line shows a single-component blackbody fit ($T = 1000$ K) to the *H* and *K'*-band detections from day 461 (note that this fit has zero degrees of freedom). The IR evolution is slow, and the detection from day 723 indicates the degree of fading in the NIR. The SED shows a rapid decline toward the red portion of the optical, as well as a strong rise toward the red within the NIR. These characteristics are precisely those predicted by the IR and scattered-light echo models.

bluer than the spectrum at peak. Indeed, the ~ 0.4 mag color change shows excellent agreement with a λ^{-1} scattering law. A λ^{-2} scattering law, on the other hand, would predict a -0.83 mag change to the $V - I$ color, or roughly $V - I \approx 0.20$ mag during the late-time epochs.

This behavior is similar to what one would expect from a scattered-light echo: as in the case of an IR echo, when successive paraboloids sweep out to progressively larger radii, dust in the circumstellar (or in some cases the interstellar) environment can scatter that light toward the observer, creating a plateau in the optical light curve of the SN. At the same time, scattering preferentially selects shorter wavelengths, which results in a spectrum that is bluer than that of the SN at peak. This is the precise behavior observed for the Type Ia SNe 1991T (Schmidt et al. 1994), 1998bu (Cappellaro et al. 2001), and 2006X (Wang et al. 2008), which all showed significant departures from the expected decline rate of SNe Ia. Spectra taken roughly two years after maximum, for SNe 1991T and 1998bu, and ~ 10 months after maximum for SN 2006X, show emission features similar to those seen in the spectra near peak superposed on top of a blue continuum for these SNe. Light echoes have also been observed around a number of core-collapse SNe, such as SN 2003gd (Sugerman 2005; Van Dyk, Li, & Filippenko 2006), SN 1993J (Sugerman & Crots 2002), and SN 1987A (see Sugerman et al. 2005, and references therein).

In Figure 7 we show the late-time SED of SN 2006gy, including our NIR detections on days 461 and 723 and the optical detections from day 810. The solid blue line represents a single-component blackbody at $T = 12,000$ K, roughly the peak temperature of SN 2006gy (Smith et al. 2010), normalized to our *F814W* detection. The SED clearly shows that the late-time emission is significantly bluer than a blackbody spectrum. We note

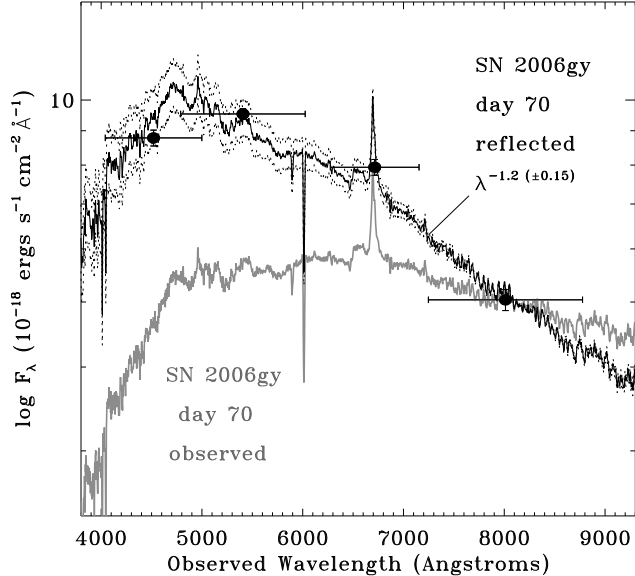


FIG. 8.— Evidence for a scattered-light echo from the blue optical emission from SN 2006gy. The *HST*/WFPC2 photometry of SN 2006gy (black dots) is compared to observed and reflected spectra, both normalized to the *HST* *F814W* flux density. The gray line is the observed spectrum of SN 2006gy on day 70 during its peak luminosity phase, from Smith et al. (2010). We plot the observed wavelength (i.e., not corrected for the SN redshift), and the spectrum has no correction for reddening. The black line (and dotted lines above and below) show the same spectrum, but adopting an assumed wavelength dependence for the dust reflectance proportional to $\lambda^{-1.2(\pm 0.15)}$.

that the early-time spectra of SN 2006gy show considerable line blanketing blueward of ~ 4000 Å, such that the emission decreases blueward of our *F450W* detection. The NIR emission rapidly rises toward the IR, suggesting that there is considerable IR emission to which our NIR measurements are not sensitive.

Figure 8 illustrates the observed *HST* photometry on day 810, as well as the observed spectrum (grey solid line) of SN 2006gy obtained near peak luminosity (Smith et al. 2010). The observed late-time photometry is clearly bluer than the spectrum at the time of peak luminosity (note that no correction for reddening has been made to either the observed spectrum or the late-time photometry). The blue colors at late times are difficult to explain with ongoing CSM interaction because SNe II_n typically exhibit relatively constant temperatures of ~ 6000 – 6500 K at late times (e.g., Smith et al. 2010), which would be redder than the spectrum at peak which had a temperature of $\sim 12,000$ K. A bluer color would be expected, however, if the optical emission at the time of peak luminosity is reflected by dust grains with a size smaller than the observed wavelength, which leads to the spectrum characterized by a $\lambda^{-\alpha}$ scattering law, as mentioned above. Figure 8 shows that the observed spectrum from day 71 can be modified by a scattering law with $\alpha = 1.2 \pm 0.15$ to adequately model the late-time *HST* photometry. We do not have a late-time spectrum to confirm that the observed line strengths are consistent with the reflected peak luminosity, and so this precludes a more detailed model of the scattering dust at this time.

3.4. Location of the Scattering Dust

The location of the scattering dust is of interest as it can help determine properties of the environment local to SN 2006gy. In Section 3.2.4 we show that the CSM dust responsible for the NIR echo cannot account for all the reddening observed toward SN 2006gy, suggesting that the SN light passes through external, non-CSM dusty regions in the host galaxy prior to reaching us. Therefore, the scattered-light echo could originate in a number of different locations.

With only a single epoch of the unresolved scattered-light echo, a precise determination of the location of the scattering dust cannot be obtained. Nevertheless, we can gain some insight into the dust location based on the total optical and NIR emission. For the case where the NIR-echo dust also gives rise to the scattered-light echo, and assuming the SN can be modelled as a single short pulse of UV/optical radiation, the ratio of the scattered-light luminosity (L_s) to the IR luminosity at late times can be shown to be (Chevalier 1986)

$$\frac{L_s}{L_{\text{IR}}} = \frac{\omega}{1 - \omega} \left(1 - \frac{(ct)^2}{4R_2^2} \right) \frac{(1 - g)^2}{2g^2} \times \left\{ \frac{(1 - g)^2 + 2g}{[(1 - g)^2 + 4g]^{1/2}} - \frac{(1 - g)^2 + gct/R_2}{[(1 - g)^2 + 2gct/R_2]^{1/2}} \right\}, \quad (4)$$

where ω is the dust albedo, c is the speed of light, t is the time since the SN explosion, R_2 is the outer radius of the dust shell, and g is a measure of the degree of forward scattering. Once again, as in Section 3.2.4 we have assumed a dust density $n_d \propto r^{-2}$. The case $g = 0$ corresponds to isotropic scattering and $g = 1$ is completely forward scattering. Note that in Equation 4 we have assumed that $ct/2 < R_1$, where R_1 is the inner radius of the dust shell, and that the albedo is independent of frequency. Empirical estimates and numerical calculations (White 1979) show $g \approx 0.6$, which we adopt here. Models and observations of interstellar dust show that for near-UV, optical, and NIR emission, which dominate the output from SN 2006gy near peak, the dust scatters light at these wavelengths with $0.4 \lesssim g \lesssim 0.7$ (see Draine 2003, and references therein). For the dust albedo we adopt $\omega \approx 0.6$ (Mathis, Ruml, & Nordsieck 1977). For the albedo, models and observations typically constrain $0.5 < \omega < 0.7$, for scattered near-UV, optical, and NIR light (Draine 2003). As mentioned above, we cannot constrain R_2 with our current observations, but we do know that R_2 must be greater than R_1 , and the value of Equation 4 does not change when $R_2 \rightarrow \infty$. For reasonable limits to the outer radius, $1.5R_1 < R_2 < \infty$, we find that $L_s/L_{\text{IR}} \approx 0.88$ – 0.60 .

Direct integration of the *HST* optical flux, which extends from ~ 4500 – 8000 Å, yields an optical luminosity of $\sim (7.4 \pm 0.5) \times 10^7 L_{\odot}$. This value is somewhat uncertain because our data do not extend into the UV; however, optical spectra taken near peak show that line blanketing severely reduces the flux blueward of ~ 4000 Å (Smith et al. 2010), so this uncertainty should not have a significant effect on the total scattered-light luminosity. If we assume that the NIR flux continues to decline at the same rate as that observed between days 398 and 723, then assuming that the NIR emission peaks in the K' band (see Section 3.2), we find a lower limit to the

IR luminosity (again, because our NIR observations only probe emission from the hottest dust) of $L_{\text{IR}} > 8.6 \times 10^7 L_{\odot}$ on day 810. Therefore, on day 810, $L_s/L_{\text{IR}} < 0.86$, consistent with the predicted values above in the case where the scattering dust is the same dust responsible for the IR echo.

The alternative possibility is that the scattering dust is not located in the CSM, instead existing at some other location in NGC 1260 along the line of sight. Cappellaro et al. (2001) inferred that this was the case with SNe 1991T and 1998bu, and like those two SNe we know that SN 2006gy has a significant amount of dust located along the line of sight. As shown by Cappellaro et al. (2001), if we approximate the SN light curve as a short pulse with duration Δt_{SN} , then the scattered-light luminosity is

$$L_{\text{echo}}(t) = L_{\text{SN}} \Delta t_{\text{SN}} f(t), \quad (5)$$

where $L_{\text{SN}} \Delta t_{\text{SN}}$ can be obtained via direct integration of the observed light curve, $L_{\text{SN}} \Delta t_{\text{SN}} = \int_0^{+\infty} L_{\text{SN}}(t) dt$, and $f(t)$ is the fraction of light scattered to the observer. Under the assumption that light is being scattered by dust in a sheet of thickness $\Delta D \ll D$, where D is the distance between the dust and the SN, then (Chevalier 1986; Cappellaro et al. 2001)

$$f(t) = \frac{c}{8\pi} \frac{\omega\tau}{D + ct} \frac{1 - g^2}{\{1 + g^2 - 2g[D/(D + ct)]\}^{3/2}}, \quad (6)$$

where τ is the optical depth of the dust. Using the relation $A_V = 1.086\tau_V$, and the fact that A_V outside the dusty CSM is ~ 1.6 mag, we find $\tau \approx 1.5$. From Smith et al. (2010), we know that $L_{\text{SN}} \Delta t_{\text{SN}} \approx 2.5 \times 10^{51}$ erg. Therefore, using $L_{\text{echo}} \approx 2.9 \times 10^{41}$ erg s $^{-1}$, from the direct integration of the optical SED, we find (from Equation 6) that dust located at $D \approx 20$ pc can explain the observed scattered-light luminosity. This value for D is dependent upon our assumptions about the albedo and the degree of forward scattering, g . To show how D changes based on these assumptions, we show D as a function of g for fixed values of the albedo $\omega = 0.3, 0.4, 0.6,$ and 0.9 in Figure 9. The large red point shows the solution for our assumed values of $g = 0.6$ and $\omega = 0.6$. We also shade the area corresponding to the expected range of values for g and ω mentioned above. This shaded area corresponds to $D \approx 10$ – 40 pc, as the location of the scattering dust.

Our observations appear to be consistent with one of two scenarios: either (i) the scattered-light echo is due to CSM dust, which has also been heated and is radiating in the IR, or (ii) a dusty region ~ 10 – 40 pc from the SN is responsible for the late-time optical luminosity. This latter scenario seems very plausible if the progenitor of SN 2006gy was a very massive star, $\gtrsim 100 M_{\odot}$ (Smith et al. 2010). If this were the case, we might expect that the progenitor resides in the center of a giant H II region with multiple dense, dusty clouds nearby. This scenario might be very similar to the Carina nebula surrounding η Car, which has multiple dusty molecular clouds only 10–20 pc from η Car (e.g., Smith & Brooks 2007). If the progenitor of SN 2006gy were surrounded by such a nebula, then our assumption of a single, thin

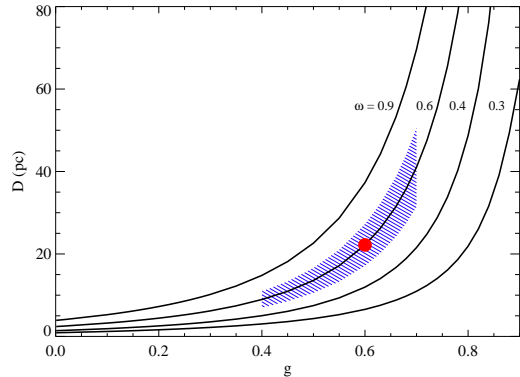


FIG. 9.— Location of the scattering dust, D , as a function of the degree of forward scattering, g , for various values of the albedo, ω . The large red point highlights our adopted values of $g = 0.6$ and $\omega = 0.6$, which corresponds to $D \approx 20$ pc. The shaded area encompasses the full range of values expected for the scattering of near-UV, optical, and NIR light by interstellar dust, $0.4 < g < 0.7$ and $0.5 < \omega < 0.7$ (see text). The shaded area corresponds to $D \approx 10$ – 40 pc. Note that this figure only applies to the case where the scattering grains are external, and unrelated, to the dust giving rise to the NIR echo.

scattering surface would no longer be valid, and the scattering dust could potentially be located at a number of different locations.

With only a single epoch of observations, we cannot distinguish between the two possible dust locations. One additional epoch of optical imaging should prove sufficient to determine which scenario is correct. As long as $D \gg ct$, then $f(t)$ is roughly constant, whereas the models of Chevalier (1986) show a continuous decline in the scattered-light echoes when $g = 0.6$ and the scattering dust is in the CSM. A relatively flat optical light curve would put the dust at ~ 20 pc, whereas significant decline from the observed day 810 flux would suggest CSM dust. Finally, we note that the prospects for fully resolving the SN 2006gy light echo are dim: at a distance of 73 Mpc it would take several decades before the light echo could be resolved with high spatial resolution images (i.e., comparable to *HST* in the optical).

4. CONCLUSIONS AND FUTURE WORK

We have presented new observations of SN 2006gy, including early-time NIR data from PAIRITEL, as well as optical and NIR detections more than two years after explosion. These new data, combined with other late-time observations, provide evidence for IR and scattered-light echoes, as follows.

1. There is no radio or X-ray counterpart to SN 2006gy, suggesting that CSM interaction is weak or nonexistent at late times.
2. There is (statistically weak) evidence for a growing NIR excess around day ~ 100 .
3. The decline of both the optical and NIR emission is slower than that of ^{56}Co , which rules out a pair-instability SN as the cause of the extreme peak optical luminosity for SN 2006gy.
4. Emission from warm dust explains the red NIR color, while an IR echo is needed to explain the long-lived NIR emission.

5. The late-time optical emission has a bluer spectrum than the SN at peak optical emission, which can be explained with a scattered-light echo.

Given our interpretation for the late-time optical and NIR emission arising from a dust shell at $\sim 8 \times 10^{17}$ cm from the SN, what might we expect from future observations of SN 2006gy? The IR-echo models of Dwek (1983) show that after a time $t \approx 2R_1/c$, the IR luminosity falls off the plateau and exhibits significant decline. Based on our predicted value for the size of the dust-free cavity (see §3.2.2), we would expect that the plateau phase of the IR echo has ended, and that the IR flux is now in steady decline. Future observations of this decline will place limits on the outer extent of the dust shell, which will in turn provide better limits on the total mass of the dust shell. Our ability to predict the behavior of the scattered-light echo is limited by the current degeneracy concerning the physical location of the scattering dust. If the same dust is responsible for both the IR and scattered-light echoes, then we would expect that the optical emission is now fading, in a manner similar to what ought to be seen in the NIR. Our observations are also consistent with dust located at ~ 10 – 40 pc from the SN, in which case we might expect the scattered-light echo to continue at roughly a constant flux for several more years. Continued observations with *HST* would allow us to distinguish between these two situations.

The shell-shock model of Smith & McCray (2007) may also explain the peak luminosity of several other VLSNe: SNe 2005ap, 2006tf, 2008es (Quimby et al. 2007; Smith et al. 2008a; Miller et al. 2009; Smith et al. 2010). This model requires large CSM densities at a distance of a few $\times 10^{15}$ cm, which can be accomplished if the SN progenitor undergoes significant (~ 0.1 – $1 M_{\odot} \text{ yr}^{-1}$) mass loss during the few decades prior to explosion. The most luminous LBVs have observed mass shells with $\gtrsim 10 M_{\odot}$ (Smith & Owocki 2006, and references therein), indicative of giant eruptions (Humphreys & Davidson 1994) but not LBVs in their more typical state with less violent wind variability (see Smith, Vink, & de Koter 2004 for a general reference on LBV winds). The possible connection between large CSM densities and VLSNe may suggest that their progenitors are LBVs (Smith et al. 2010). Furthermore, the direct identification of the progenitor of the Type IIIn SN 2005gl showed it to be an LBV (Gal-Yam et al. 2007; Gal-Yam & Leonard 2009), which strengthens the connection between SNe IIIn and LBV progenitors. For the case of SN 2006gy, Smith et al. (2008b) argue that the dusty shell at $\sim 10^{18}$ cm could exist if the progenitor underwent an LBV-like eruptive mass-loss phase ~ 1200 yr prior to the SN. IR echoes for other VLSNe have not been reported to date, but we strongly encourage a search for them. If a substantial fraction of them exhibit late-time characteristics similar to SN 2006gy, this may be suggestive of a common timescale, ~ 1000 yr and ~ 10 yr, for extreme mass loss

in the progenitors of VLSNe. The combination of a VLSNe and IR echo would point to multiple phases of eruptive mass loss, which is reminiscent of LBV behavior. The instability driving these eruptions still remains unclear (one possibility is the pulsation pair instability described by Woosley, Blinnikov, & Heger 2007 to explain SN 2006gy), and we encourage future observational and theoretical work to better characterize these systems.

We thank Schuyler Van Dyk for his assistance in the preparation of the *HST* snapshot proposal. Andy Becker, Maryam Modjaz, Dovi Poznanski, and the anonymous referee provided many useful suggestions that helped to improve this paper. We thank Cullen Blake, Dan Starr, and Emilio Falco for their assistance in the operation of PAIRITEL.

This publication makes use of data products from the Two Micron All Sky Survey, which is a joint project of the University of Massachusetts and the Infrared Processing and Analysis Center/California Institute of Technology, funded by the National Aeronautics and Space Administration (NASA) and the National Science Foundation (NSF).

A.A.M. is supported by the NSF Graduate Research Fellowship Program. J.S.B.’s group is partially supported by NASA/*Swift* grant #NNG05GF55G and a Hellman Faculty Award. A.V.F.’s SN group at UC Berkeley is grateful for support from NSF grants AST-0607485 and AST-0908886, the TABASGO Foundation, and NASA grants AR-11248 and GO-10877 from the Space Telescope Science Institute, which is operated by AURA, Inc., under NASA contract NAS 5-26555. J.X.P. is partially supported by NASA/*Swift* grant NNX07AE94G and NSF CAREER grant AST-0548180. The Peters Automated Infrared Imaging Telescope is operated by the Smithsonian Astrophysical Observatory (SAO) and was made possible by a grant from the Harvard University Milton Fund, the camera loan from the University of Virginia, and the continued support of the SAO and UC Berkeley. The PAIRITEL project is partially supported by NASA/*Swift* Guest Investigator Grant #NNG06GH50G. KAIT and its ongoing operation were made possible by donations from Sun Microsystems, Inc., the Hewlett-Packard Company, AutoScope Corporation, Lick Observatory, the NSF, the University of California, the Sylvia & Jim Katzman Foundation, and the TABASGO Foundation. Some of the data presented herein were obtained at the W. M. Keck Observatory, which is operated as a scientific partnership among the California Institute of Technology, the University of California, and NASA; it was made possible by the generous financial support of the W. M. Keck Foundation. The authors wish to recognize and acknowledge the very significant cultural role and reverence that the summit of Mauna Kea has always had within the indigenous Hawaiian community; we are most fortunate to have the opportunity to conduct observations from this mountain.

REFERENCES

- Abel, T., Bryan, G. L., & Norman, M. L. 2000, *ApJ*, 540, 39
 Agnoletto, I., et al. 2009, *ApJ*, 691, 1348
 Barkat, Z., Rakavy, G., & Sack, N. 1967, *PRL*, 18, 379
 Barris, B. J., et al. 2005, *AJ*, 130, 2272
 Bietenholz, M., & Bartel, N. 2008, *ATel*, 1657, 1

- Bloom, J. S., et al. 2006, in *Astronomical Data Analysis Software and Systems XV*, ed. C. Gabriel, et al. (San Francisco: ASP, vol. 331), 751
- Bond, J. R., Arnett, W. D., & Carr, B. J. 1984, *ApJ*, 280, 825
- Cappellaro, E., et al. 2001, *ApJ*, 549, L215
- Cardelli, J. A., Clayton, G. C., & Mathis, J. S. 1989, *ApJ*, 345, 245
- Chevalier, R. A. 1986, *ApJ*, 308, 225
- Chugai, N. N., & Danziger, I. J. 1994, *MNRAS*, 268, 173
- Cohen, M., Wheaton, W. A., & Megeath, S. T. 2003, *AJ*, 126, 1090
- Dolphin, A. E. 2000, *PASP*, 112, 1397
- Draine, B. T. 2003, *ARA&A*, 41, 241
- Draine, B. T. & Li, A. 2001, *ApJ*, 551, 807
- Dwek, E. 1983, *ApJ*, 274, 175
- Filippenko, A. V. 1997, *ARA&A*, 35, 309
- Filippenko, A. V., et al. 2001, in *Small-Telescope Astronomy on Global Scales*, ed. W. P. Chen, C. Lemme, & B. Paczyński (San Francisco: ASP, vol. 246), 121
- Fox, O., et al. 2009, *ApJ*, 691, 650
- Gal-Yam, A., & Leonard, D. C. 2009, *Nature*, 458, 865
- Gal-Yam, A., et al. . 2007, *ApJ*, 656, 372
- Gal-Yam, A., et al. . 2009, *Nature*, 462, 624
- Ganeshalingam, M. 2009, private communication
- Gerardy, C. L., et al. 2002, *ApJ*, 575, 1007
- Gezari, S., et al. 2009, *ApJ*, 690, 1313
- Holtzman, J. A., et al. 1995a, *PASP*, 107, 156
- Holtzman, J. A., et al. 1995b, *PASP*, 107, 1065
- Humphreys, R. M., & Davidson, K. 1994, *PASP*, 106, 1025
- Kawabata, K. S., et al. 2009, *ApJ*, 697, 747
- Koekemoer, A. M., Fruchter, A. S., Hook, R. N. & Hack, W. 2002, in *The 2002 HST Calibration Workshop: Hubble after the Installation of the ACS and the NICMOS Cooling System*, ed. S. Arribas, A. Koekemoer, & B. Whitmore (Baltimore, MD: Space Telescope Science Institute), 337
- Li, W., et al. 2002, *PASP*, 114, 403
- Li, W., et al. 2003, *ApJ*, 586, L9
- Li, W., et al. 2010, *ApJ*, in prep.
- Mathis, J. S., Rumpl, W., & Nordsieck, K. H. 1977, *ApJ*, 217, 425
- Miller, A. A., et al. 2009, *ApJ*, 690, 1303
- Nadyozhin, D. K. 1994, *ApJS*, 92, 527
- Nomoto, K., et al. 2007, in *Supernova 1987A: 20 Years After: Supernovae and Gamma-Ray Bursters*, ed. S. Immler, K. Weiler, & R. McCray (New York: AIP, vol. 937), 412
- Ofek, E. O., et al. 2007, *ApJ*, 659, L13
- Pozzo, M., et al. 2004, *MNRAS*, 352, 457
- Quimby, R. M., et al. 2007, *ApJ*, 668, L99
- Rakavy, G., & Shaviv, G. 1967, *ApJ*, 148, 803
- Riess, A. G., et al. 1999, *AJ*, 118, 2675
- Scannapieco, E., et al. 2005, *ApJ*, 633, 1031
- Schlegel, E. M. 1990, *MNRAS*, 244, 269
- Schmidt, B. P., et al. 1994, *ApJ*, 434, L19
- Skrutskie, M. F., et al. 2006, *AJ*, 131, 1163
- Smith, N., & Brooks, K. J. 2007, *MNRAS*, 379, 1279
- Smith, N., Chornock, R., Silverman, J., Filippenko, A. V., & Foley, R. J. 2010, *ApJ*, in press (arXiv:0906.2200)
- Smith, N., Foley, R. J., & Filippenko, A. V. 2008, *ApJ*, 680, 568
- Smith, N., & McCray, R. 2007, *ApJ*, 671, L17
- Smith, N., & Owocki, S. P. 2006, *ApJ*, 645, L45
- Smith, N., Vink, J. S., & de Koter, A. 2004, *ApJ*, 615, 475
- Smith, N., et al. 2007, *ApJ*, 666, 1116
- Smith, N., et al. 2008a, *ApJ*, 686, 467
- Smith, N., et al. 2008b, *ApJ*, 686, 485
- Smith, N., et al. 2009, *ApJ*, 695, 1334
- Spitzer, L., Jr. 1978, *Physical Processes in the Interstellar Medium* (New York: Wiley-Interscience)
- Sugerman, B. E. K. 2005, *ApJ*, 632, L17
- Sugerman, B. E. K., & Crotts, A. P. S. 2002, *ApJ*, 581, L97
- Sugerman, B. E. K., et al. 2005, *ApJ*, 627, 888
- Van Dyk, S. D., Li, W., & Filippenko, A. V. 2006, *PASP*, 118, 351
- Wang, X., et al. 2008, *ApJ*, 677, 1060
- White, R. L. 1979, *ApJ*, 229, 954
- Wizinowich, P. L., et al. 2006, *PASP*, 118, 297
- Woosley, S. E., Blinnikov, S., & Heger, A. 2007, *Nature*, 450, 390
- Yuan, F., et al. 2008, *ATel*, 1389